CHARACTERISATION OF Al-COMPOUND REFRACTIVE LENSES FOR X-RAYS

F. Ewald, J.-C. Biasci, ESRF, Grenoble, France

Abstract

We report on measurements of the surface quality (shape) of aluminium compound refractive lenses using a thin collimated X-ray beam from one of our bending magnet diagnostics beam ports. Two types of lenses were tested for overall radius of curvature, surface quality and thickness: commercially available lenses (RWTH Aachen), and lenses of the same type manufactured at the ESRF. The different surface qualities can be readily discerned with our relatively simple setup. While the technique should be improved for more precise results, it already shows clearly the imperfect surface structure of the ESRF lenses. The image quality of the beam, however, is not affected to a visible extent in our emittance measurement setup at vertical emittances of typically ~ 6 pm.

INTRODUCTION

In order to characterise the quality of some aluminium lenses made at the ESRF we performed beam deflection and absorption measurements at our pinhole beam port ID25 as well as imaging and phase contrast measurements at the beamline ID6. These measurements allow to assess the overall parabolic shape, the surface structure and the apex thickness of the lenses. They are always compared to the same measurements performed with lenses purchased from RWTH Aachen.

For a detailed description of X-ray lenses and their properties see [1], [2] and references therein. Here we just recall the expression for the focal length of a stack of N single lenses with radius of curvature R and the energy-dependent index of refraction $\delta(E)$:

$$f = \frac{R}{2N\delta(E)} \quad . \tag{1}$$

This relation is correct provided that individual focal lengths f_i and distances between lenses d_i are such that $f_\mathrm{i} \gg d_\mathrm{i}$. This condition holds, because $d_\mathrm{i} = 2$ mm while $f_\mathrm{i} = 96.06$ m.

By the geometry of the setup, the focal length is fixed by the distances between source and lens $g = (4.525 \pm 0.001)$ m and between lens and screen $b = (12.483 \pm 0.002)$ m, respectively (see Fig. 1):

$$f = (\frac{1}{g} + \frac{1}{b})^{-1} = (3.3211 \pm 0.0007)\ \mathrm{m} \quad . \tag{2}$$

The number of lenses used during the tests were $N = 29$ (RWTH Aachen) and $N = 23$ (ESRF), corresponding theoretically through equation 1 to the energies 45.62 keV and 40.63 keV, respectively. If – and only if – the source is located at the position of a (vertical) beam waist, a sharp image and the corresponding energy can experimentally be found by scanning the (vertical) image size as function of the energy. The minimum then corresponds to the energy that fulfills equations 1 and 2. For the source point at the beam port ID25 the waist is located $X = 6$ mm downstream the -1.5 mrad X-ray source position (see [3] for explanation). The resulting optimum energies were found at 45.5 keV (RWTH Aachen) and 40.4 keV (ESRF). The energy resolution of the monochromator had been determined previously. It is 0.02 keV, and the absolute energy is calibrated within this precision using the K absorption edge of Sn. With $\sim$ 0.25 keV the uncertainty in the determination of the minimum energy from the energy scan is considerably higher than the precision of the monochromator itself. This is due to the flat minimum and the noise level. The total error of the measurement of the energy energy minimum is thus roughly $\Delta E_\mathrm{exp} = 0.3$ keV.

Parabolicity, Surface Quality, Radius of Curvature

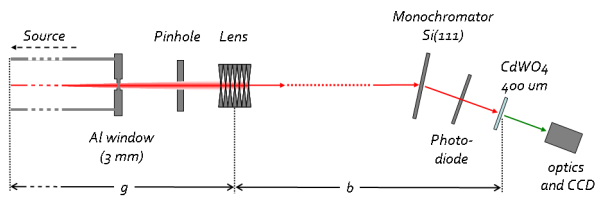

Figure 1: Setup of the measurements performed at the bending magnet beam port ID25. The X-ray beam is collimated with the help of the pinhole that is installed in front of the lens (the usual pinhole for emittance measurement). The lens can then be scanned across the beam for focal length or absorption measurements.

In order to probe locally the lens surface, the dipole radiation was collimated using the pinhole situated in front of the lens (see Fig. 1). Two pinhole sizes are available which create pencil beams on the lens of either 15 μm $\times$ 65 μm or 7.5 μm $\times$ 65 μm (vertical $\times$ horizontal). It has to be noted that the footprint of the probing beam size is large at the steep walls of the parabolically shaped lens. The recorded signal is therefore always an average over a lens surface area greater than the probe beam size itself. Since the pinhole is wide in the horizontal plane, no scans in this plane are performed, and the vertical scans contain an average over a horizontal stripe of roughly 70 μm. The first measurements were done with the wide vertical pinhole (15 μm). The lens was then scanned vertically across the

ISBN 978-3-95450-127-4

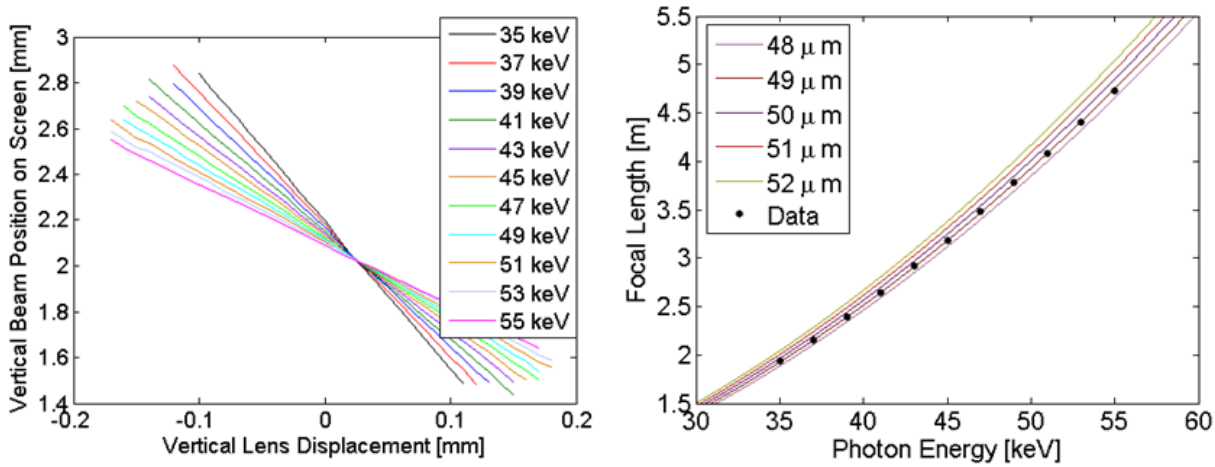

Figure 2: Lenses from RWTH Aachen: Beam movement on the scintillating screen as function of vertical lens displacement for different photon energies (left plot) and measured focal length (black dots in the right plot), deduced from the slopes of the beam displacement shown in the left plot. The lines show the theoretical focal lengths for different radii of curvature R of the parabola.

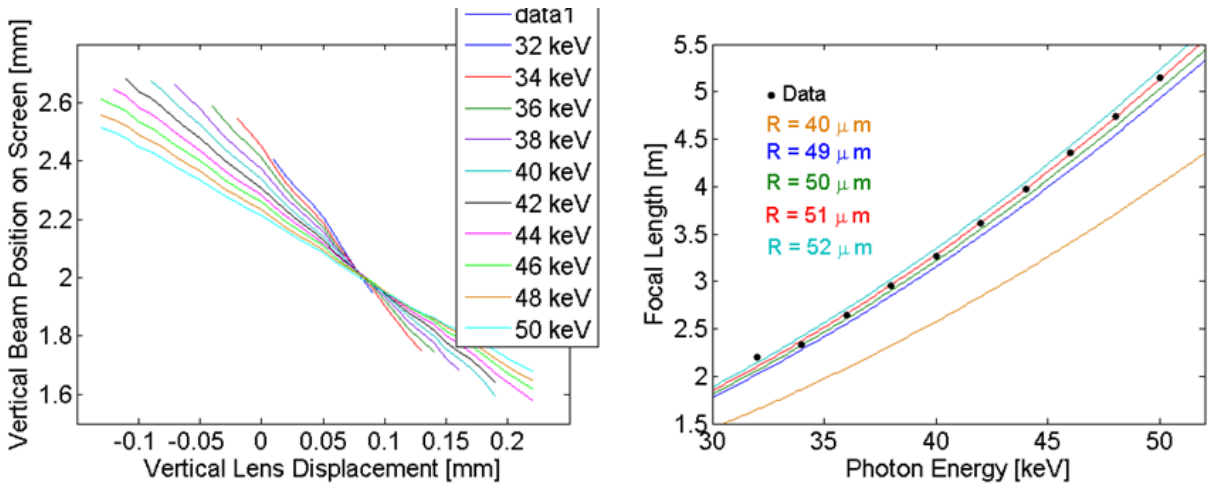

Figure 3: Results of the beam deflection measurement of the ESRF lenses, using a probe beam size of 14 μm in the vertical plane. Explanations of the plot as in the text and in Fig. 2.

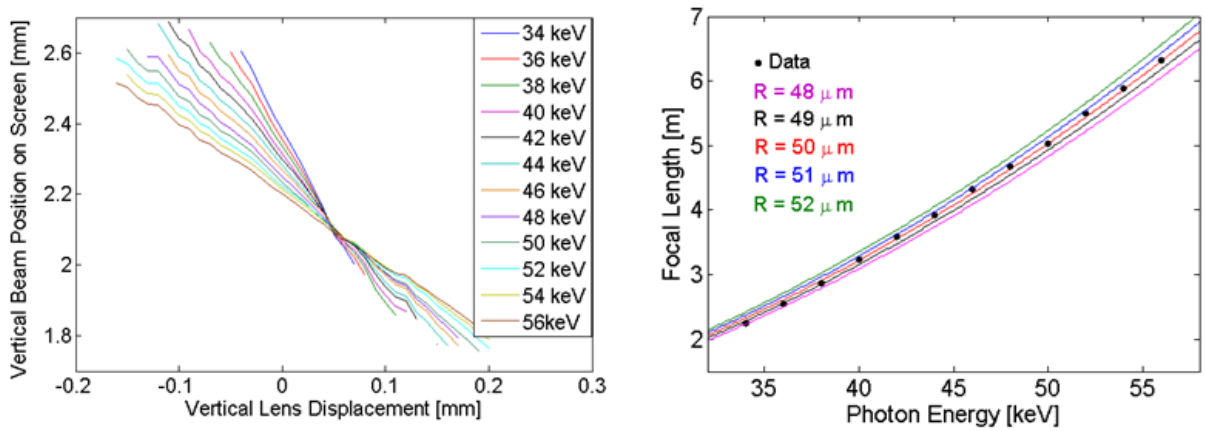

Figure 4: Beam deflection scans and focal length measurement for the ESRF lens. In comparison to Fig. 3 the probing X-ray beam size (in the vertical plane) is reduced using the small vertical pinhole of 7 μm size.

ISBN 978-3-95450-127-4

beam. For an ideal parabola the dependence between beam deflection and lens movement shall be strictly linear. If the lens surface abberrates from the parabolic shape, the deflection will deviate from linearity. The left plots in Figs. 2 and 3 show the deflection scans for several photon beam energies. The array of lenses from RWTH Aachen shows an impressively linear behaviour, proving the nearly perfect parabolic shape of these lenses. Instead, the ESRF lenses show some deviations from linearity, even if the overall deflection is linear. This indicates some defects on the otherwise parabolic shape. It has to be noted that for the RWTH Aachen lenses we do not know if there is a fixed orientation of the lenses with respect to the forming tool. As a consequence, the individual lenses are randomly oriented. Potential systematic defects in the lenses may then average out. For the ESRF lenses, however, the orientation during the forming procedure is fixed and a reference hole in the lens frame allows to align all lenses with the same orientation in the beam. Defects generated by the forming tool will therefore superpose and can be pin pointed.

From a linear fit of the deflection data, the overall slope can be deduced, ignoring the local defects (which however contribute to the quality of the fit). The focal length of the lens set is then simply:

$$f_{\mathrm{defl}} = -\frac{b}{\mathrm{slope}} \quad , \tag{3}$$

where b is the distance between lens and detector (scintillator screen). Of course, f_{defl} depends on the photon energy. In the right plots of Figs. 2 and 3 f_{defl} is plotted as function of the photon energy together with the focal length f calculated from the index of refraction, radius of curvature and number of lenses. For the set of RWTH Aachen lenses the measured focal length lies perfectly on the theoretical line for lenses with a radius of curvature of $R = 49\ \mu\mathrm{m}$ for all photon energies, while the ESRF lenses fit better to a radius of curvature of $R = 51\ \mu\mathrm{m}$. The two points corresponding to the lowest energies are not to be taken into account, because the data are not sufficiently good due to the strong absorption of the lenses at 32 and 34 keV. Due to the strong deviation from linearity of the slopes, the radius of curvature cannot be determined with a better precision than $\sim 2\ \mu\mathrm{m}$.

A second scan (only for the ESRF lenses) was done using the narrower 7 μm pinhole. Tiny defects in the lens can be resolved better in this case as can be seen in Fig. 4. Indeed, the deviations from parabolicity which were already visible with the lower resolution scan are more pronounced.

Since the deflection scans can be done only in the vertical direction due to the extended pinhole size in the horizontal plane, a new measurement was done with the lenses turned by $90°$. If the defects on the lenses are not rotationally symmetric, the deflection scans should be different from those done at $0°$. Indeed, the defects (data not shown) appear at different locations after rotation.

Absorption Scans – Determination of Lens Apex Thickness

The transmission of the collimated X-ray beam through the lens was measured as function of the beam position on the lens using the total flux on the camera. The measurement was done, using the polychromatic beam. In parallel the transmission through the lens is modeled by calculating the absorption through N concave parabolic aluminium lenses with the radius of curvature of $R = 50\ \mu\mathrm{m}$. The apex distance of the parabola is then adapted until the modeled transmitted flux fits the data. The best fit is found for $d = 20\ \mu\mathrm{m}$ (RWTH Aachen) and $d = 110\ \mu\mathrm{m}$ (ESRF). This corresponds very well to the expectations, the RWTH Aachen lenses being specified for $d = 24\ \mu\mathrm{m}$ and the ESRF lenses having a thick apex due to the non-perfect forming tool.

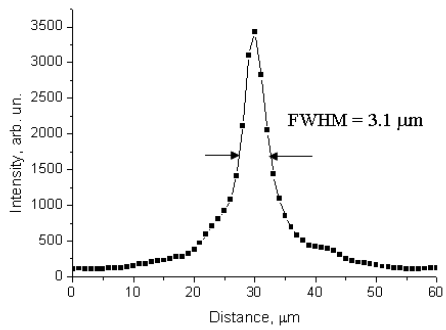

Figure 5: Vertical profile of the X-ray beam imaged at the beamline ID6. The X-ray energy was 12.5 keV and a stack of $N = 5$ lenses was used.

Imaging Quality and Phase Contrast Images

Additionally to the measurements at the dipole beam port ID25 we had the possibility to test the lenses at the beamline ID6. A number of $N = 5$ lenses is needed to image the source ($E = 12.4$ keV, $g = 55$ m, $b = 1.25$ m). Figure 5 shows the vertical profile of the focused X-ray beam. Theoretically, the vertical focus size should be

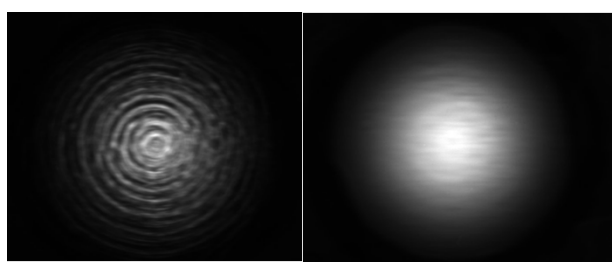

Figure 6: Phase contrast images of a single lens (camera positioned out of focus). Left, a lens made at the ESRF. Right, a lens from RWTH Aachen.

ISBN 978-3-95450-127-4

2.27 μm (taking into account the demagnification, and imaging resolution). The real measured beam size is 3 μm and the profile shows clearly an asymmetric shape with broad tails and shoulders, which indicates imperfections of the parabolic lens shape. Turning the lens stack by 90°, the profile changes (no image shown here), confirming the systematic shape errors due to the forming tool. The overall shape of the lens is nevertheless good, as is confirmed by the comparison of the measured effective aperture of 90 μm compared to the ideal 95 μm obtained from calculation (data not shown).

Finally, a phase contrast image of a single lens reveals the traces of the milling cutter left on the forming tool and then imprinted on the lens (Fig. 6). They were already perceptible by eye and are the most probable reason for the observed abberations. The absence of any perceptible surface structure on the Aachen lens sets the target for further improvements in the lens making.

CONCLUSIONS

All the performed measurements show that the overall shape of the first lenses fabricated at the ESRF is already acceptable. They have indeed, as aimed for, a radius of curvature of 50 μm within the precision of the measurements (2 μm). However, the "fine structure" of the lens surfaces deviates locally from the parabolic shape, giving rise to abberations. For any serious X-ray imaging application these abberations will have to be removed. Likewise the apex thickness needs to be reduced, else the absorption of a lens stack will be too important. An improvement of the forming tool will allow these two improvements.

ACKNOWLEDGEMENTS

The authors would like to thank A. Snigirev and I. Snigireva for many instructive discussions and the measurements at the beamline ID6.

REFERENCES

[1] P. Elleaume, "Optimization of compound refractive lenses for X-rays", Nuclear Instruments and Methods in Physics Research A, 412, p. 483 (1998).

[2] B. Lengeler, J. Tümmler, et al. "Transmission and gain of singly and doubly focusing refractive X-ray lenses", Journal of Applied Physics, 84, p. 5855 (1998).

[3] F. Ewald, et al. "Emittance measurement using X-ray lenses at the ESRF", IBIC'13, Oxford, WEPF11, (2013).

ISBN 978-3-95450-127-4